

Peri-Urban to Urban Landscape Patterns Elucidation through Spatial Metrics

Ramachandra T.V.^{1, 2, 3,*}, Bharath Setturu¹ and Bharath H. Aithal^{1, 2}

¹Energy & Wetlands Research Group, Centre for Ecological Sciences [CES],

²Centre for Sustainable Technologies (astra)

³Centre for infrastructure, Sustainable Transportation and Urban Planning [CiSTUP]
Indian Institute of Science, Bangalore, Karnataka, 560 012, India

Abstract—Elucidation of urban land use dynamics with the quantification and pattern analysis of spatial metrics is gaining significant importance in recent times. Rapid unplanned urbanisation has telling impacts on natural resources, local ecology and infrastructure. Analysing spatio-temporal characteristics of urban landscapes through remote sensing data and landscape metrics will help in evolving appropriate strategies for integrated regional planning and sustainable management of natural resources. Temporal remote sensing data provides an opportunity to identify, quantify spatio-temporal changes. This helps in the implementation of location specific mitigation measures to minimize the impacts. This Communication focuses on spatio temporal patterns of the land use dynamics of Bangalore. Analysis was carried out radially from the city center using temporal remote sensing data acquired through space-borne sensors. Greater Bangalore with 10 kilometer buffer is considered in order to take into account spatial changes in the gradient of peri-urban to urban regions. The region has been divided into eight zones based on directions. Further, these zones are divided into 13 circles each of 2 km radius (Bangalore administrative region: 741 square kilometer being 16 km radius with 10 kilometer buffer), Landscape metrics was computed for each circle in each zone, which helped in understanding spatio-temporal patterns and associated dynamics of the landscape at local levels. PCA and CCA analysis were carried out that helped in prioritising metrics for understanding the interrelationships of spatial patterns while eliminating redundancy of numerous indices in the landscape level analysis. The analysis reveals there has been a growth of 28.47 % in urban area of Bangalore metropolitan region (including 10 kilometer buffer) during 1973 to 2010. Landscape metrics analysis reveals compact growth at the center and sprawl in the peri-urban regions.

Keywords—Urban, Landscape metrics, Shannon entropy, UII, GRASS.

I. INTRODUCTION

Urbanisation is a dynamic process refers to the growth of urban population resulting in land use land cover (LULC) changes, being experienced by most of the developing nations. Recent projections indicate that the world population living in urban areas will reach 60 percentages by 2030 [1]. Urbanisation process involves changes in LULC, socioeconomic aspects including population density. Urban land use entails interactions of urban economic activities with environment, which further leads to expansion. The rapid and uncontrolled growth of the urbanising cities brings numerous changes in the structure and hence the functioning of landscape [2]. Urban form reveals the relationship between a city with its surroundings as well as the impact of human actions on the local environment within and around a city [3]. This necessitates planning at various stages to manage the urban growth while addressing economic development with the environment goals. Multi Resolution remote sensing data acquired through sensors mounted on Earth Observation Satellites (EOS) provides a synoptic and repetitive coverage of large areas through time. It is now possible to monitor and analyze urban expansion and land use changes in a timely and cost-effective way due to improvements in spatial, spectral, temporal and radiometric resolutions with analytical techniques [4]. However, there are technical challenges in retrieving accurate information of urban expansions with rapid land use changes. A major challenge in urban remote sensing data analysis is caused by the high heterogeneity and complexity of the urban environment in terms of its spatial and spectral characteristics. A successful implementation of remote sensing technique requires adequate consideration and understanding of these specific urban landscape characteristics in order to explore the capabilities and limitation of remote sensing data and to develop appropriate image analysis techniques [5]. Recently there has been an increased interest in the application of spatial metrics techniques in urban environment because of their capability in revealing the spatial component in landscape structure with the dynamics of ecology and growth process [6-9]. The analysis of temporal landscape structure would aid in accounting spatial implications of ecological processes [10]. Many spatial landscape properties can be quantified by using a set of metrics [5], [11-14]. In this context, spatial metrics are a very valuable tool for planners in understanding and accurately characterising urban processes and their consequences [5], [10], [15]. Spatial metrics have aided in landscape monitoring, including landscape changes [16-18], assessing impacts of management decisions and human activities [19-21]. A variety of landscape metrics have been proposed to characterize the spatial configuration of individual landscape class or the whole landscape base [22-25]. Compared to the other change detection techniques, the landscape metrics techniques are advantageous in capturing inherent spatial structure of landscape pattern and biophysical characteristics of these spatial dynamic [26]. Furthermore, spatial metrics have the potential for detailed analyses of the spatio-temporal patterns of urban change, and the interpretation and assessment of urbanisation process.

Land use dynamics detection using remote sensing data

Remote sensing data aids in detecting and analysing temporal changes occurring in the landscape. Availability of digital data offers cost effective solutions to map and monitor large areas. Remote sensing methods have been widely applied in mapping land surface features in urban areas [27]. Satellite based remote sensing offers a tremendous advantage over historical maps or air photos, as it provides consistent observations over a large geographical area, revealing explicit patterns of land cover and land use. It presents a synoptic view of the landscape at low cost [28]. Remote sensing also provides high-resolution datasets that are used to assess spatial structure and pattern through spatial metrics.

Landscape metrics analysis for landscape change detection

Landscape metrics or spatial metrics is based on the geometric properties of the landscape elements, are indicators widely used to measure several aspects of the landscape structure and spatial pattern, and their variation in space and time [12]. A variety of landscape metrics have been proposed to characterize the spatial configuration for the individual landscape class or the whole landscape. Scaling functions of the images describes the variations of different landscape pattern metrics with spatial resolutions [29-31]. Patch size and patch shape metrics have been widely used to assess patch fragmentation both at small and large scales [26]. Patch shape index acts as an indicator, which correlates with the basic parameter of individual patch, such as the area, perimeter, or perimeter–area ratio. However, these indices fail in reflecting the spatial location of patches within the landscape [25]. Heterogeneity based indices proposed subsequently aid in quantifying the spatial structures and organization within the landscape which was not quantified by patch shape index. Similarly, the proximity indices quantify the spatial context of patches in relation to their neighbors [32]. For example, the nearest-neighbor distance index distinguishes isolated distributions of small patches from the complex cluster configuration of larger patches [33]. Thus patch-based and heterogeneity-based indices highlight two aspects of spatial patterns, which are complement to each other. As landscape patterns possess both homogeneous and heterogeneous attributes, it is necessary to adopt both groups of indices for analysing spatial patterns of heterogeneous landscapes [34]. This illustrates that multi-resolution remote sensing data with spatial metrics provide more spatially consistent and detailed information about urban structures with the temporal changes, while allowing the improved representations for better understanding of heterogeneous characteristics of urban areas. This helps in assessing the impacts of unplanned developmental activities on the surrounding ecosystems.

II. OBJECTIVES

Main objective of the study is to quantify urbanisation process. This involved,

- a. Quantitative assessment of the spatio-temporal dynamics of urbanising landscape.
- b. Analysis of urbanisation process through spatial metrics.

III. STUDY AREA

Greater Bangalore with an area of 741 square kilometers and with an altitude of 949 meters above sea level is the administrative capital of Karnataka State, India is located in the Deccan Plateau to the south-eastern part of Karnataka. It lies between the latitudes 12°39'00" to 13°13'00"N and longitude 77°22'00" to 77°52'00"E. To account for rural-urban gradient, 10 kilometer circular buffer has been considered from the Bangalore administrative (<http://www.bbmp.gov.in/>) boundary by considering the centroid as City Business District (CBD).

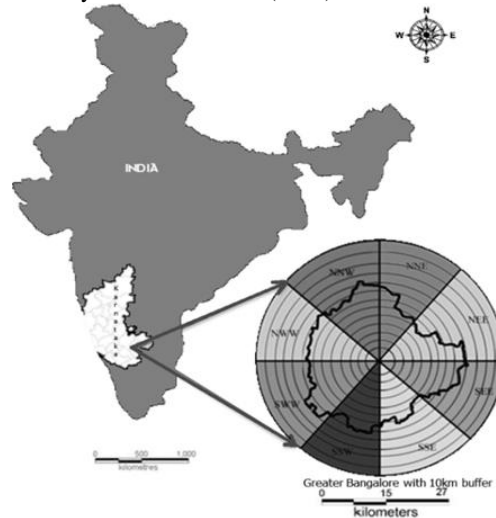


Fig.1 Study area

Bangalore was founded in the year 1537 by then ruler Kempe Gowda and has eventually evolved into economic hub of Karnataka. Bangalore is accessible by air, road, and rail. The city is well-known for its diverse culture, and history. Greenery with salubrious climate has attracted a large number of investors and migrants from other parts of the country as well as from overseas. Bangalore has grown ten folds spatially from 69 (1949) to 741 square kilometer [35]. Bangalore has been witnessing rapid urbanisation since 1990's, which has resulted in fundamental land use changes. 632% increase in

built-up has resulted in the loss of 76% vegetation and 78% water bodies during the last four decades. These large scale landscape changes has influenced the local climate and has aided in regular floods, Bangalore has been experiencing changes in the temperature leading to urban heat islands [36].

IV. MATERIALS

Remote sensing data

Multi-resolution remote sensing data of Landsat (a series of earth resource scanning satellites launched by the USA) satellite for the period 1973 to 2010 has been used. The time series of Landsat Series Multispectral sensor (57.5 meter) of 1973, Thematic mapper (28.5 meter) sensors for the years 1992 and 1999, Enhanced Thematic Mapper Plus (30 meter) of 2003, 2008 and 2010, were downloaded from public domain USGS (<http://glovis.usgs.gov/>) and GLCF (<http://glcf.umiacs.umd.edu/data>). Survey of India (SOI) topo-sheets of 1:50000 and 1:250000 scales were used to generate base layers of city boundary, etc. City map with ward boundaries were digitized from the BBMP (Bruhat Bangalore MahanagaraPalike) map. Ground control points to register and geo-correct remote sensing data were collected using pre-calibrated handheld GPS (Global Positioning System) and Google earth (<http://earth.google.com>).

V. METHOD

Figure 2 outlines the method adopted for analysing multi-resolution remote sensing data. Landsat data acquired were geo-corrected with the help of known ground control points (GCP's) collected from the Survey of India topo-sheets and Global Positioning System (GPS). ETM+ data was corrected for SLC-off defect. Geo corrected data is then resampled to 30 meter in order to maintain a common resolution across all the data sets.

The data was classified into four land use categories - urban, vegetation, water bodies and others (open space, barren land, etc.) with the help of training data using supervised classifier – Gaussian maximum likelihood classifier (GMLC). This preserves the basic land use characteristics through statistical classification techniques using a number of well-distributed training pixels. **Grass GIS**(<http://wgbis.ces.iisc.ernet.in/grass/index.php>), free and open source software with robust support of processing both vector and raster data has been used for this analysis. Possible errors during spectral classification are assessed by a set of reference pixels. Based on the reference pixels, statistical assessment of classifier performance including confusion matrix, kappa (κ) statistics and producer's and user's accuracies were calculated. These accuracies relate solely to the performance of spectral classification. Infill, linear, clustered, expansion, scattered are considered as different growth types in this study. Infill development is usually referred as compact development. Infill development converts vacant or unutilized urban land into higher density development. Infill is means of accommodating the growth within urban area's geographical extent. Growth of the urban is modeled by a fixed amount of changes for each time period referred as linear growth. The expansion of a community without concern for consequences and expanded around their peripheries that forms a new agglomeration termed as high expansion or clustered growth. Scattered development is a low density development, growth of urban area increases dramatically in short time span with new development activities in the periphery.

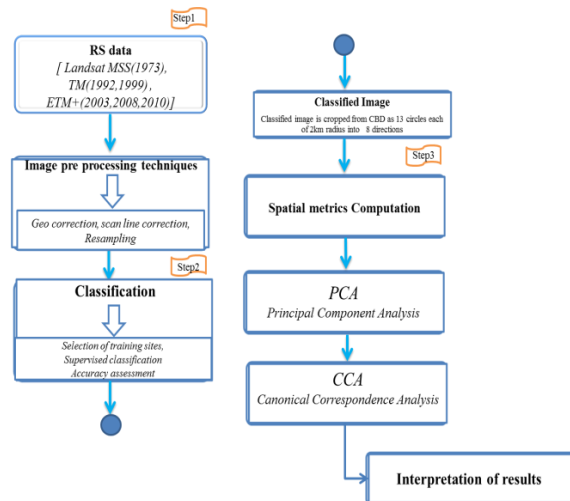


Fig. 2 Method tailored to understand urban landscape change

Analysis of urban sprawl

Urban sprawl refers to the disaggregated or dispersed growth at outskirts and these localities are devoid of basic amenities (drinking water, sanitation, etc.). This necessitates understanding sprawl process for effective regional planning. The location factors, such as distance to urban center and roads act as catalyst for urban sprawl. Shannon's entropy given in equation 1 has been used to measure the extent of urban sprawl with remote sensing data [37], [38]. Shannon's entropy was calculated across all directions to analyse the extent of urbanisation

$$H_n = - \sum P_i \log_e(P_i) \dots \dots \dots (1)$$

Where, P_i is the Proportion of the variable in the i^{th} zone and n is the total number of zones. This value ranges from 0 to $\log n$, indicating very compact distribution for values closer to 0. The values closer to $\log n$ indicates that the distribution is much dispersed. Larger value (close to $\log n$) indicates fragmented growth indicative of sprawl.



Fig. 3 Study area with important landmarks (source: Google Earth)

Analysis of spatial patterns of urbanisation - computation of Landscape metrics

The gradient based approach is adopted to explain the spatial patterns of urbanisation. The study region, given in Figure 1 was divided into eight zones based on the directions, which were further divided into concentric circles (13 circles) with incrementing radius of 2 kilometer. Landscape metrics were computed for each region to understand the landscape dynamics at local levels due to urbanisation.

A Spatio-temporal pattern of the landscape is understood through landscape metrics. These spatial metrics are a series of quantitative indices representing physical characteristics of the landscape mosaic. Table 1(Appendix I) lists the indicators that reflect the landscape’s spatial and temporal changes [5], [16], [39], [40]. These metrics are grouped into the five categories: Patch area metrics, Edge/border metrics, Shape metrics, Compactness/ contagion / dispersion metrics, Open Space metrics.

Analysis of land use expansion – computation of Urban Intensity Index (UII):

Urban Intensity Index (UII) is used to compare the intensity of land use expansion at different time periods. UII results in the normalization of the land area in various spatial units divided by the annual rate of expansion [41]. UII is the percentage of expansive area of urban land use in the total area and is given by 2.

$$UII = [(UA_{i,t+n} - UA_{i,t})/n] * [100/TA] \dots\dots (2)$$

Where UA is urban area per year of spatial unit i, urban land use area of year t+n, land use of year t and TA resembles total land area;n represents the number of years.

VI. RESULTS AND DISCUSSION

Temporal land use changes are given in Table 2. Figures 4 and 5 depict the temporal dynamics during 1973 to 2010. This illustrates that the urban land (%) is increasing in all directions due to the policy decisions of industrialization and consequent housing requirements in the periphery. The urban growth is concentric at the center and dispersed growth in the periphery. Table 3 illustrates the accuracy assessment for the supervised classified images of 1973, 1992, 1999, 2003, 2008 and 2010 with an overall accuracy of 93.6%, 79.52%, 88.26%, 85.85%, 99.71%, and 82.73%.

Table 2 illustrates that the percentage of urban has increased from 1.87(1973) to 28.47% (2010) whereas the vegetation has decreased from 62.38 to 36.48%.

Table 2.a: Temporal land use of Bangalore in %

| Land use Type→ | Urban | Vegetation | Water | Others |
|----------------|-------|------------|-------|--------|
| Year | % | % | % | % |
| 1973 | 1.87 | 62.38 | 3.31 | 32.45 |
| 1992 | 8.22 | 58.80 | 1.45 | 31.53 |
| 1999 | 16.06 | 41.47 | 1.11 | 41.35 |
| 2003 | 19.7 | 38.81 | 0.37 | 41.12 |
| 2008 | 24.94 | 38.27 | 0.53 | 36.25 |
| 2010 | 28.97 | 36.48 | 0.79 | 34.27 |

Table 2.b: Temporal land use of Bangalore in hectares

| Land use → | Urban | Vegetation | Water | Others |
|------------|----------|------------|---------|----------|
| Year | Ha | Ha | Ha | Ha |
| 1973 | 3744.72 | 125116.74 | 6630.12 | 65091.6 |
| 1992 | 17314.11 | 123852.87 | 3063.69 | 66406.5 |
| 1999 | 32270.67 | 83321.65 | 2238.21 | 83083.05 |
| 2003 | 39576.06 | 77985.63 | 748.26 | 82611.18 |
| 2008 | 50115.96 | 76901.94 | 1065.42 | 72837.81 |
| 2010 | 57208.14 | 73286.46 | 1577.61 | 68848.92 |

Table 3: Accuracy assessment

| Year | Kappa coefficient | Overall accuracy (%) |
|------|-------------------|----------------------|
| 1973 | 0.88 | 93.6 |
| 1992 | 0.63 | 79.52 |
| 1999 | 0.82 | 88.26 |
| 2003 | 0.77 | 85.85 |
| 2008 | 0.99 | 99.71 |
| 2010 | 0.74 | 82.73 |

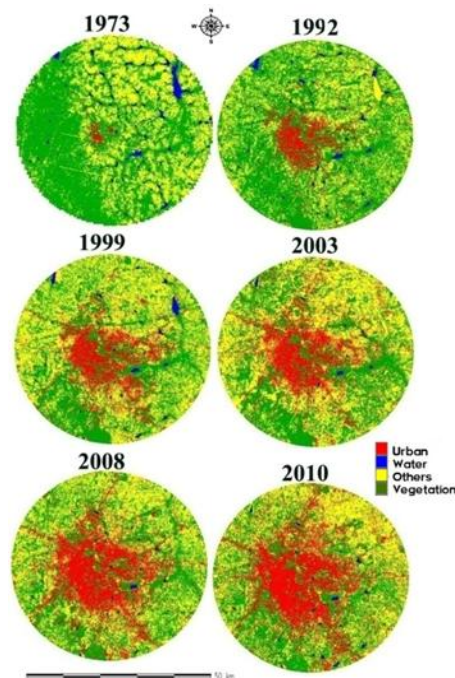


Fig. 4 Bangalore from 1973, 1992, 1999, 2003, 2008 and 2010

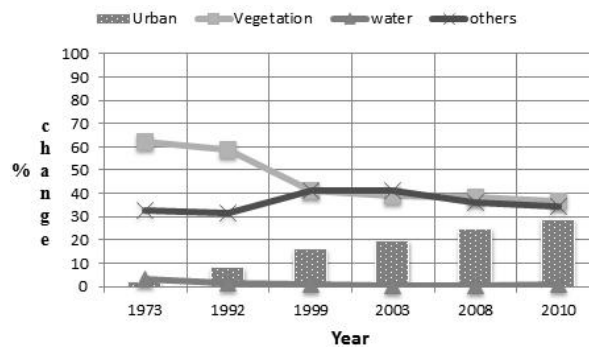


Fig. 5 Land use dynamics for Bangalore from 1973 to 2010

Land use Dynamics of Bangalore from 1973-2010

Figure 6 (in Appendix II) explains the spatio temporal land use dynamics of Greater Bangalore with 10 kilometer buffer region for the period 1973 to 2010. The built-up percentage (urban) in circle 1 is increasing (from 1973 to 2010) in all directions with the decline of vegetation. In 1973 built-up is high in NNE (25.37%), NWW (17.45%), NNW (43.25%) directions whereas in 2010 built-up has increased in NNE (79.02%), SSW (74.11%), NWW (76.89%), NNW (85.71%) directions due to compact growth of residential areas, commercial complex areas. *Infilling* is observed in these regions during 1973 to 2010 due to conversion of open spaces and vegetated areas into built-up. The urban land is increasing in all directions in Circle 2, due to more residential areas like Shantinagar, Majestic, Seshadripuram etc.,. In 1973 built-up is high in SSW (11.33%), SWW (47.05%), NWW (18.96%) directions whereas in 2010 built-up has increased in NNE (90.00%), SSW (78.25%), SWW (78.30%) directions, declining the vegetation cover in the region. In 1973 built-up is high in SSW (39.94%), NWW (33.03%) directions in Circle 3 whereas in 2010 built-up has increased substantially in NNE (89.24%), SSW (71.06%), SWW (92.06%), NWW (83.73%), NNW (69.39%) directions, which in turn show decline of vegetation cover in the region. The urban land has increased in all directions due to increase in residential and commercial areas like Gandhinagar, Guttahalli, Wilson Garden, KR Market, Kormangala (some of the IT industries are located in this region) etc. It has been observed *infilling* urban growth in the region due to more commercial/financial services/activities. Land use changes in the circle 4 during 1973 to 2010 indicate an increase of urban land in all directions due to dense residential areas like Malleswaram, Rajajinagar, Jayanagar, Yeshwanthpur and small scale industries estates like Rajajinagar Industrial area, Yeshwanthpur Industrial suburb etc.,. In the year 1973 built-up percentage is high in SEE (5.06%) and NWW (7.81%) directions whereas in 2010 built-up is more in NEE (77.06%), SSW (89.69%), SWW (92.39%), NWW (83.61%) directions, which in turn declining in the area of vegetation cover and water bodies in the region. In 1973, the area under built-up is less in all the direction in Circle 5 whereas in 2010, built-up has increased substantially in SSW (84.02%), SWW (93.01%), NWW (83.03%) directions, decreasing the vegetation cover.

The urban land has increased in all directions due to the increase in residential and commercial areas like Vijaynagar, Dasarahalli, Banshankari, Marthahalli, BTM layout and Bommanahalli industrial area (IT & BT industries) etc., in 1973 built-up in Circle 6 in NNW is 2.67% compared to all directions. In 2010 built-up has increased in SSW (68.12%), SWW (53.46%), NWW (66.90%) directions. The urban land is increasing in all directions due to more residential areas and commercial areas like Vidyananyapuram, Jalahalli, Yelahanka satellite Town, HMT layout etc. Asia's biggest Industrial area-Peenya Industrial estate located in this region (SWW, NWW). *Infilling* (Peenya Industries) and high expansion (other areas) is observed in this region.

The urban land is increasing with respect to all the directions due to residential area development as in Yelahanka new town, White Field, Tunganagar, MEI housing colony and small scale industries. In 1973 built-up in Circle 7 is very less, However, this has increased in 2010, in SSE (38.54%), SSW (37.72%), SWW (46.37%), NWW (63.71%) directions, which has resulted in the decline of vegetation cover and water bodies. In this region urban growth expansion due to manufacturing industrial activities is observed.

The built-up area is increasing all the directions from 1973 to 2010 in circle 8. Built-up direction wise are NNE (31.68%), SSE (32.90%), NWW (46.29%), NNW (32.29%) due to residential layouts and small scale industries.

The built-up area is increasing all the directions from 1973 to 2010. In 2010 Built-up area with respect to SSE (24.26%), SSW (21.26%), NWW (24.61%) directions has increased due to new residential areas of moderate density (Hoskote residential area) and industries (part of Bommasandra Industrial area). The built-up has increased from 1973 to 2010 in Circle 10. In 2010, Built-up has increased with respect to NNE (18.57%), SSE (22.46%), NWW (18.06%) directions due to small residential layouts, industries (part of Bommasandra Industrial area) of technical, transport and communication infrastructure. The built-up has increased in Circle 11 from 1973 to 2010 due to the land use changes from open spaces and land under vegetation to built-up. Small scale Industries near Anekal (SSE) is driving these changes. In 2010 Built-up percentage is high in NNE (16.48%), SSE (22.39%), NNW (13.35%) directions. Regions in Circle 12, in all directions have experienced the decline of water bodies and vegetation due to large scale small residential layouts and Jigani Industrial estate (located in SSE). The built-up has increased from 1973 to 2010, evident from the growth in SSE (22.09%), NNE (14.92%) and NEE (14.17%) directions during 2010.

Similar trend is observed in Circle 13 with the built up increase in SSE (21.43%), NNE (18.74%) directions due to small residential layouts, part of Jigani Industrial estate (SSE) and also residential complexes due to the proximity of Bengaluru International Airport (NNE).

Shannon's entropy

The entropy calculated with respect to 13 circles in 4 directions is listed in table 4. The reference value is taken as Log (13) which is 1.114 and the computed Shannon's entropy values closer to this, indicates of sprawl. Increasing entropy values from 1973 to 2010 shows dispersed growth of built-up area in the city with respect to 4 directions as we move towards the outskirts and this phenomenon is most prominent in SWW and NWW directions.

Table 4: Shannon entropy

| Direction | NNE | NEE | SEE | SSE | SSW | SWW | NWW | NNW |
|-------------|-------------------------------|-------|-------|-------|-------|-------|-------|-------|
| 1973 | 0.061 | 0.043 | 0.042 | 0.036 | 0.027 | 0.059 | 0.056 | 0.049 |
| 1992 | 0.159 | 0.122 | 0.142 | 0.165 | 0.186 | 0.2 | 0.219 | 0.146 |
| 1999 | 0.21 | 0.21 | 0.23 | 0.39 | 0.35 | 0.34 | 0.33 | 0.24 |
| 2003 | 0.3 | 0.25 | 0.27 | 0.33 | 0.36 | 0.4 | 0.45 | 0.37 |
| 2008 | 0.3 | 0.27 | 0.34 | 0.46 | 0.45 | 0.48 | 0.48 | 0.37 |
| 2010 | 0.46 | 0.32 | 0.38 | 0.5 | 0.5 | 0.5 | 0.54 | 0.44 |
| Year | Reference value: 1.114 | | | | | | | |

Landscape metrics Analysis and interpretation

The entropy values show of compact growth in certain pockets and dispersed growth at outskirts. In order to understand the process of urbanisation, spatial metrics (Table 1 in Appendix I) were computed. Metrics computed at the class level are helpful for understanding of landscape development for each class. The analysis of landscape metrics provided an overall summary of landscape composition and configuration.

Figure 7 to 15 (Appendix III) describes Patch area metrics. Figure 7 reflects the direction-wise temporal built-up area, while Figure 8 explains percentage of built-up. These figures illustrate the inner circles (1, 2, 3, and 4) having the higher values indicates concentrated growth in the core areas especially in SWW and NWW regions. However, there has been intense growth in all zones and in all circles inside the boundary from 1973 to 2010 and which leading to spread near the boundary and 10 kilometer buffer. The values of urban intensification in certain pockets near periphery suggest the implications of IT sector after 90’s (example: one such is the IT sector being established in the NEE & SEE regions). Patch indices (such as largest patch) is computed to understand the process of urbanisation as it provides an idea of aggregation or fragmented growth. Figure 9 and 10 shows largest patch index with respect to built-up (i.e. class level) and also with respect to the entire landscape.

In 1973, circle-3 of SWW direction has largest built-up patch, which is aggregating to form a single patch. In 2010 largest patches can be found in circle 4 to circle 12 indicating the process of urbanisation. In circle 12 with respect to all directions the largest patches are located due to new paved surfaces areas, among all NNW direction is having higher largest patch. Similar trend has been noticed for the largest patch with respect to whole landscape, which indicates of largest patch in SWW (circle 3) among one of the land use classes in 1973 and in NNE (circle 9) in 2010. In order to analyse the dimension of the urban patch and its growth intensity, Mean patch size (MPS) is computed, Results are as shown in Figure 11. MPS values are higher near the periphery in 1973 due to a single homogeneous patch. Whereas, it showed higher value near the center where urban patches were prominent and were less near periphery which indicated fragmented growth in the center in 2010.

Figure 12 shows number of patches (NP) of built-up area from 1973 to 2010. This is fragmentation based indices. Less NP in 1973 has increased in 2010 showing more fragmented patches which can be attributed to the sprawl at periphery (circle 6 to 13) with respect to all the directions. The more number of patches can be found in NNE direction of circle 6 and circle 12. The PD and NP indices are proportional to each other. Figure 13 shows patch density (PD) in built-up, which indicates lower values in 1973 and higher values in 2010 indicating fragmentation towards periphery. Figure 14 shows Patch area distribution coefficient of variation (PAD_CV) which indicates almost zero value (all patches in the landscape are the same size or there is only one patch) in 1973 with respect to all the directions in outer circles. This has been changed in 2010, with high PAD_CV indicating new different size patches in the landscape are present due to the intensified growth towards the outskirts with respect to all the directions. Figure 15 shows PAFRAC (Perimeter-Area Fractal Dimension) index from 1973 to 2010, which approaches 1 in all the directions, indicating of simple perimeters in the region.

Figure 16 to 20 (Appendix III) explains the Edge metrics to analyse the edge pattern of the landscape. Figure 16 shows Edge Density (ED), which shows an increase from circle 4 to 13 with respect to all directions from 1973 to 2010 clarifies the landscape is having simple edges at center and becoming complex to the periphery due to large number of edges or fragments in the periphery. Figure 17 shows prominent AWMPFD in 2010 for the circle 4 in all directions. Circle 5 to Circle 8 in NNW approaches to value 2, which shows the shapes of the patches are having the convoluted perimeters. AWMPFD approaches to 1 for the shapes with simple perimeters, Perimeters that are simple indicate that there is homogeneous aggregation happening in this region. Perimeters that are complex shaped indicate the fragment that are being formed, which is most prominent in 2010.

Figure 18 shows PARA_AM, which illustrates fragmentation in the outer circles with higher values in all directions for all years and especially circle 11 of NNW direction has higher perimeter. Figure 19 and 20, shows MPFD (Mean Patch Fractal Dimension), covariance indicates that in 1973 the landscape with simple edges (almost square) has become complicated in 2010 with convoluted edges in all directions because of fragmentation and newly developing edges in the landscape.

Figure 21 to 23(Appendix III) explains the shape complexity of the landscape by the utility of shape metrics. NLSI (Normalized Landscape Shape Index) which explain shape complexity of simple (in 1973) to complex in 2010 as shown in Figure 21 with respect to all directions. Figure 22 and Figure 23 shows MSI (Mean Shape Index) and AWMSI (Area Weighted Mean Shape Index) indices, which explains in 1973 the shape of landscape is simple i.e. almost square and in 2010 due to irregular patches the shape has become more complex in all directions of the outer circles.

Figure 24 to 28 (Appendix III) describes the clumpiness of the landscape in terms of the urban pattern. Figure 24 shows Clumpy Index. City is more clumped/Aggregated in the center with respect to all directions but disaggregated towards periphery indicates small fragments or urban sprawl. Circles 1, 2, 3 are clearly portraits the intensified growth of the region in respective directions.

Figure 25 shows higher ENN_AM (Euclidean nearest neighbour distance Area weighted mean) for 1973 which has reduced in all directions from 1973 to 2010 due to intermediate urban patches. The new industries and other development activities from 1992 to 2010 especially lead to establish new urban patches which lead to reduction of nearest neighbor distance of urban patches.

Figure 26 shows ENN_CV (Euclidean nearest neighbour distance coefficient of variation) Index from 1973 to 2010, which is another form of ENN_AM, and is expressed in terms of percentage. ENN_CV value is decreasing due to more unique intermediate urban patches coming up in the region with new built-up areas. Figure 27 illustrates AI (Aggregation) Index, which is similar to Figure 24 (clumpy index).

Figure 28 shows IJI (Interspersion and Juxtaposition) which is a measure of patch adjacency IJI values are increasing due to decrease in the neighbouring urban patch distance in all the directions in 2010 which is indicative of patches/fragments becomes a single patch i.e. maximal interspersion and equally adjacent to all other patch types that are present in the landscape.

Figure 29 and 30(Appendix III) explains the open space indices, computed to assess the status of the landscape for accounting the open space and dominance of land use classes. Figure 29 shows Ratio of Open Space (ROS), which helps to understand the growth of urban region and its connected dynamics. ROS was higher in 1973 with respect to all the directions, especially in the periphery of 10 kilometerboundary. ROS decreases in the subsequent years and reaches dismal low values in 2010. Specifically, circles 1, 2, 3, 4 shows the zero availability of open space indicating that the urban patch dominates the open area which causes limits spaces and congestion in the core urban area leading to the destruction of vegetation cover for construction purposes. This is also driving the migration from the city center towards periphery for new developmental activities. Figure 30 shows dominance index which increases considerably since 1973 and reaches considerably maximum value (in 2010) indicating that the urban category becoming the dominant land use in the landscape.

Finally, UII was calculated, which explains the growth rate at which the study area is urbanising temporally through years 1973 to 2010. The growth rate during 1973 to 1992 showed less intensification of urban whereas from 1992 to 2010 there has been a drastic increase. Table 5 explains the urban intensification temporally, revealing higher growth rates in NNE, NWW and NNW

Table 5: UII with respect to the previous time period

| Direction | | NNE | NEE | SEE | SSE | SSW | SWW | NWW | NNW |
|------------------|------------------|------|------|------|------|------|------|------|------|
| Year | 1973-1992 | 0.26 | 0.19 | 0.26 | 0.33 | 0.45 | 0.45 | 0.51 | 0.26 |
| | 1992-1999 | 0.43 | 0.71 | 0.76 | 2.19 | 1.51 | 1.22 | 1.11 | 0.78 |
| | 1999-2003 | 1.36 | 0.06 | 0.62 | 0.04 | 0.33 | 1.18 | 2.25 | 2.17 |
| | 2003-2008 | 0.04 | 0.35 | 1.06 | 1.27 | 1.43 | 1.33 | 0.56 | 0.27 |
| | 2008-2010 | 6.1 | 1.66 | 1 | 1.29 | 2.05 | 0.96 | 2.61 | 2.35 |

Principal components analysis (PCA):

Principal component analysis (PCA) was carried out to reduce the number of dimensions in the data set while keeping best of the variance, and to identify the major independent dimensions of the landscape patterns [42], [43]. PCA is for reduction and interpretation of large multivariate data sets [44] with some underlying linear structure. PCA is adopted in landscape analysis to identify independent components of landscape structure, and cluster analysis to group the components and then calculated the universality, strength, and consistency of the identified landscape structure components [45]. PCA helped in prioritising representative spatial metrics that best reflect the landscape’s temporal changes.

PCA has removed effect of landscape composition, and the resulting components that are the major independent dimensions of landscape configuration. Plot of principal components (PC’s) in Figure 31 shows the combination of the categories with loadings. This contains the plotted component scores of each sample and the loading coefficients as eigenvectors. The largest percentage of variance was explained by metrics from PC1 and PC2. Principal component analysis illustrates the spatial pattern of patches. The combined PCA gives the most consistent metrics with high loadings across the landscape. The positive loadings explain the behaviour of fragmentation for respective circles and also compactness in some circles. These metrics are effective for discerning the patterns of urban growth at a landscape.

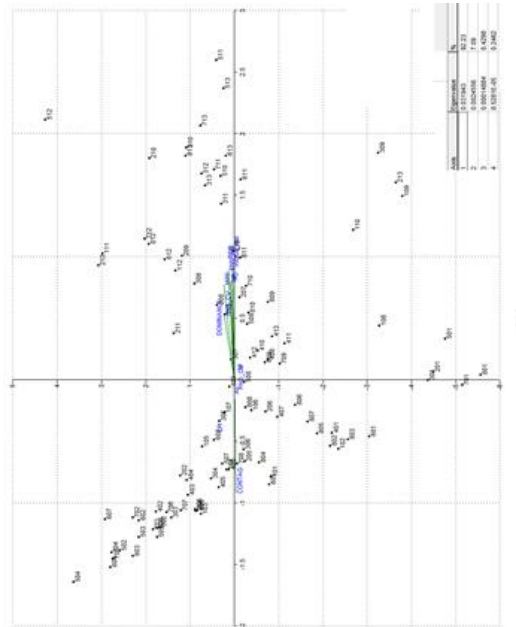


Fig. 32 CCA plot of the first and second axes with % variance

VII. CONCLUSION

The peri urban to urban gradients analysis elucidated the changes in land use intensity due to the policy focus on setting up industries, leading to the increase in the population of urban and suburbs. The study shows that Bangalore is rapidly expanding with a significant increase in built-up area from 1.87% (1973) to 28.47% (2010), whereas the vegetation has decreased from 62.38% to 36.48% and also depletion of large water bodies and open spaces. Shannon entropy value is increasing from 1973 to 2010 and reaching towards the critical (reference) value highlights the sprawl. The present work demonstrates the usefulness of spatial metrics for metropolitan land use planning.

The study identified the potential utility of common landscape metrics for discriminating different patterns of the spatio-temporal land use change in response to the process of urbanisation. The landscape metrics number of patches (NP) and patch density PD showing the higher fragmentation of urban patches at periphery. Due to higher the value of number of patches (NP), mean patch size (MPS) value has come down ENN_AM showing the intermediate urban patches are developed. AI is showing the urban patches are disaggregated towards periphery. AWMSI showing the patches are becoming more irregular. The results shows urban patches are more clumped at the urban center, but fragmented towards the periphery due to newly developed urban patches at the edge. Intensified urbanisation is taking place continuously at a faster rate in outer areas, bringing more area under built-up (Urban) category as revealed by metrics (dispersed growth).

PCA was implemented to prioritize the landscape metrics useful for analysing urban dynamics. CCA was also done which brought out the critical relationships between metrics and hence proved as a very useful statistical tool to explain the higher contributors in a given set of landscape metrics. Finally, urban landscape planning design requires strengthening the structural connectivity of ecological landscapes to improve urban-ecological functional linkages. Spatial metrics and variables of urban land use form the basis for alternative representations of these factors in urban models. Such information at regional level will help decision makers in modifying the landscape in order to achieve a sustainable balance of resources.

ACKNOWLEDGEMENTS

We are grateful to the Ministry of Science and Technology, Government of India, Centre for *infrastructure Sustainable Transportation and Urban Planning* [CiSTUP] and Indian Institute of Science for the financial and infrastructure support.

REFERENCES

- [1]. United Nations Report 2008. <http://www.un.org/millenniumgoals/reports.shtml>.
- [2]. Solon, J., 2009. Spatial context of urbanisation: Landscape pattern and 1950 and 1990 in the Warsaw metropolitan area, Poland. *Landscape and Urban Planning* doi:10.1016/j.landurbplan.2009.07.012.
- [3]. Grimm Nancy B, Stanley H. Faeth, Nancy E. Golubiewski, Charles L. Redman, Jianguo Wu, Xuemei Bai and John M. Briggs, 2008. Global change and the ecology of cities, *Science* 319 (5864), 756–760.
- [4]. Yang, L.M., Xian, G., Klaver, J.M., Deal, B., 2003. Urban land-cover change detection through sub-pixel imperviousness mapping using remotely sensed data. *Photogrammetry Engineering Remote Sensing*. 69, 1003–1010.
- [5]. Herold M, 2005. The role of spatial metrics in the analysis and modelling of urban land use change” *Computer, Environ, and Urban Systems* 29, 369–399.
- [6]. McGarigal K., B. Marks, 1995. FRAGSTATS, spatial pattern analysis program for quantifying landscape structure. General Technical Report PNW-GTR-351. USDA, Forest service, Pacific, Northwest research station, Portland.

- [7]. Luck, M., Wu, J., 2002. A gradient analysis of urban landscape pattern: a case study from the Phoenix metropolitan, Arizona, USA. *Landsc. Ecol.* 17, 327–339.
- [8]. Dietzel, C., Herold, M., Hemphell, J.J., Clarke, K.C., 2005. Spatio-temporal dynamics in California's central valley: Empirical links to urban theory. *Int. J. Geographic Information Science*, 19(2), 175-195.
- [9]. Porter Bolland, L., Ellis, E.A., Cholz, F.L., 2007. Land use dynamics and landscape history in La Montaña, Campeche. *Landscape and Urban Planning*, 82,198–207.
- [10]. Di Bari, J., 2007. Evaluation of five landscape-level metrics for measuring the effects of urbanisation on landscape structure: the case of Tucson, Arizona, USA. *Landscape and Urban Planning*. 79, 308–313.
- [11]. McGarigal, K., S.A. Cushman, M.C. Neel, E. Ene, 2002. FRAGSTATS: Spatial Pattern Analysis Program for Categorical Maps. Computer software program produced by the authors at the University of Massachusetts, Amherst.
- [12]. Li, H., Wu, J., 2004. Use and misuse of landscape indices. *Landsc. Ecol.* 19, 389–399.
- [13]. Uuemaa, E., Antrop, M., Roosaare, J., Marja, R., Mander, U., 2009. Landscape metrics and indices: an overview of their use in landscape research. *Living Rev. Landsc. Res.* 3, <http://www.livingreviews.org/lrlr-2009-1>.
- [14]. Herold, M., Goldstein, N.C., Clarke, K.C., 2003. The spatiotemporal form of urban growth: measurement, analysis and modeling. *Remote Sens. Environ.* 86, 286–302.
- [15]. Kim, J., Ellis, C., 2009. Determining the effects of local development regulations on landscape structure: comparison of the woodlands and North Houston, TX. *Landscape and Urban Planning*. 92, 293–303.
- [16]. Lausch A, F. Herzog, 2002. Applicability of landscape metrics for the monitoring of landscape change: issues of scale, resolution and interpretability/ *Ecological Indicators* 2, 3–15.
- [17]. Petrov, L., Lavalle, C., Kasanko, M., 2009. Urban land use scenarios for a tourist region in Europe: applying the MOLAND model to Algarve, Portugal. *Landscape and Urban Planning*. 92, 10–23.
- [18]. Ramachandra T.V., A.H. Bharath and D.S. Durgappa. Insights to urban dynamics through landscape spatial pattern analysis, *Int. J Applied Earth Observation and Geoinformation*, 18, 2012, 329- 43.
- [19]. Geri, F., Amici, V., & Rocchini, D., 2010. Human activity impact on the heterogeneity of a Mediterranean landscape. *Applied Geography*. 30(3), 370-379.
- [20]. Lin, Y., Han, G., Zhao, M., & Chang, S. X., 2010. Spatial vegetation patterns as early signs of desertification: a case study of a desert steppe in Inner Mongolia, China. *Landscape Ecology*. 10,1519-1527.
- [21]. Proulx, R., & Fahrig, L., 2010. Detecting human -driven deviations from trajectories in landscape composition and configuration. *Landscape Ecology*, 10, 1479-14 87.
- [22]. Patton, D.R., 1975. A diversity index for quantifying habitat "edge". *Wildl. Soc. Bull.* 3:171–173.
- [23]. Forman, R.T.T., Gordron, M., 1986. *Landscape Ecology*. John Wiley & Sons, New York, ISBN 0-471-87037-4.
- [24]. O'Neill, R.V., Krummel, J.R., Gardner, R.H., Sugihara, G., Jackson, B.L., DeAngelis, D.L., Milne, B.T., Turner, M.G., Zygmunt, B., Christensen, S.W., Dale, V.H., Graham, R.L., 1988. Indices of landscape pattern. *Landscape and Ecology*. 1, 153–162.
- [25]. Imbernon, J., Branthomme, A., 2001. Characterization of landscape patterns of deforestation in tropical rain forest. *Int. J. Remote Sens.* 22, 1753–1765.
- [26]. Fuller, D.O., 2001. Forest fragmentation in Loudoun County, Virginia, USA evaluated with multi temporal Landsat imagery. *Landsc. Ecol.* 16, 627–642.
- [27]. Haack, B. N., Guptill, S. C., Holz, R. K., Jampoler, S. M., Jensen, J. R., & Welch, R. A. (1997). Urban analysis and planning. In Philipson et al. (Eds.), *Manual of photographic interpretation* (2nd ed., p517–554).
- [28]. Lillesand, T.M., Keifer, R.W. 1987. *Remote sensing and Image interpretation*, John Willey and Sons, New York.
- [29]. Wu, J., Shen, W., Sun, W., Tueller, P.T., 2002. Empirical patterns of the effects of changing scale on landscape metrics. *Landscape Ecology* 17 (8), 761–782.
- [30]. Yu, X., Ng, C., 2006. An integrated evaluation of landscape change using remote sensing and landscape metrics: a case study of Panyu, Guangzhou. *International Journal of Remote Sensing* 27 (6), 1075–1092.
- [31]. Saura S, Castro S, 2007. Scaling functions for landscape pattern metrics derived from remotely sensed data: Are their sub pixel estimates really accurate? *ISPRS Journal of Photogrammetry & Remote Sensing* 62, 201–216.
- [32]. Gustafson, E.J., 1998. Quantifying landscape spatial pattern: what is the state of the art? *Ecosystems* 1,143–156.
- [33]. Turner, M.G., 1989. Landscape ecology: the effects of pattern on process. *Ann. Rev. Ecol. Syst.* 20, 171–197.
- [34]. Turner, M.G., Gardner, R.H., 1990. Quantitative method in landscape ecology: an introduction. *Ecolog. Stud.* 82, 3–14.
- [35]. Ramachandra, T.V., and Kumar, U., 2008, Wetlands of Greater Bangalore, India: Automatic Delineation through Pattern Classifiers. *Electronic Green Journal* 26, Web URL: <http://egj.lib.uidaho.edu/index.php/egj/article/view/3171>.
- [36]. Ramachandra, T.V., and Kumar, 2009. Urban Land surface temperature with land cover dynamics: multi-resolution, spatio-temporal data analysis of Greater Bangalore, *International Journal of Geo informatics*, 5(3), 43-53.
- [37]. Yeh, A. G. O., & Li, X. 2001. Measurement and monitoring of urban sprawl in a rapidly growing region using entropy. *Photogrammetric Engineering and Remote Sensing*, 67(1), 83–90.
- [38]. Sudhira, H. S., Ramachandra, T. V., & Jagdish, K. S., 2004. Urban sprawl: metrics, dynamics and modeling using GIS. *International Journal of Applied Earth Observation and Geo information*, 5, 29–39.
- [39]. Aguilera, F., Luis Valenzuela M., Andre Botequilha-Leitao., 2011. Landscape metrics in the analysis of urban land uses patterns: A case study in a Spanish metropolitan area. *Landscape and Urban Planning*, 99, 3-4, 226-238.

- [40]. Taubenbock H. M., Wegmann, A. Roth, H. Mehl, S. Dech, 2009. Urbanisation in India – Spatiotemporal analysis using remote sensing data Original Research Article Computers, Environment and Urban Systems, 33, 3, 179 - 188.
- [41]. Dong W, Zhang XL, Wang B., Duan Z.L, 2007. Expansion of Urmqi urban area and its spatial differentiation, Science in China Series D: Earth Sciences 50,159-168.
- [42]. Riitters, K.H., O'Neill, R.V., Hunsaker, C.T., Wickham, J.D., Yankee, D.H., Timmins, S.P., Jones, K.B., Jackson, B.L., 1995. A factor analysis of landscape pattern and structure metrics, Landscape Ecology, 10(1), 23-39.
- [43]. Jackson, D.A., 1993. Stopping rules in principal components analysis: a comparison of heuristical and statistical approaches. Ecology, 74, 2204–2214.
- [44]. Sabatier, R., Lebreton, J.D., Chessel, D., 1989. Principal component analysis with instrumental variables as a tool for modelling composition data, 341-352.
- [45]. Samuel, A. C., McGarigal, k., Neel, M.C., 2008. Parsimony in landscape metrics: Strength, universality, and consistency Ecological Indicators, 8 (5), 691-703.
- [46]. TerBraak, J.F.C., 1986. Canonical Correspondence Analysis: A new Eigenvector Technique for Multivariate Direct Gradient Analysis. Ecology, 67 (5), 1167-1179.
- [47]. Retuerto, R., Carballeira, A., 1991. Defining phytoclimatic units in Galicia, Spain, by means of multivariate methods. Journal of Vegetation Science, 2, 699-710.
- [48]. Palmer, M.W., 1993. Putting things in even better order – the advantages of canonical correspondence-analysis. Ecology, 74, 2215–2230.

Appendix I:

Table 1: Landscape metrics with significance

| SL NO | INDICATORS | FORMULA | RANGE | SIGNIFICANCE/ DESCRIPTION |
|--------------------------------------|---|---|-----------------------|---|
| <i>Category : Patch area metrics</i> | | | | |
| 1 | Built up (Total Land Area) | ----- | >0 | Total built-up land (in ha) |
| 2 | Built up (Percentage of landscape) | $BP = \frac{A_{builtup}}{A} (100)$ A _{built-up} = total built-up area A= total landscape area | 0<BP≤100 | It represents the percentage of built-up in the total landscape area. |
| 3 | Largest Patch Index (Percentage of built up) | $LPI = \frac{\max(a_i)}{A} (100)$ a _i = area (m ²) of patch i A= total landscape area | 0 ≤ LPI≤100 | LPI = 0 when largest patch of the patch type becomes increasingly smaller. LPI = 100 when the entire landscape consists of a single patch of, when largest patch comprise 100% of the landscape. |
| 4 | Mean patch size MPS | $MPS = \frac{\sum_{i=1}^n a_i}{n_i} \left(\frac{1}{10,000} \right)$ i=i th patch a=area of patch i n=total number of patches | MPS>0, without limit | MPS is widely used to describe landscape structure. Mean patch size index on a raster map calculated, using a 4 neighbouring algorithm. |
| 5 | Number of Urban Patches | $NPU = n$ NP equals the number of patches in the landscape. | NPU>0, without limit. | It is a fragmentation Index. Higher the value more the fragmentation |
| 6 | Patch density | f(sample area) = (Patch Number/Area) * 1000000 | PD>0, without limit | Calculates patch density index on a raster map, using a 4 neighbor algorithm. |

| | | | | |
|---------------------------------------|--|--|--|---|
| 7 | Patch area distribution coefficient of variation (PADCV) | $PAD_{CV} = \frac{SD}{MPS} (100)$ <p>with:SD: standard deviation of patch area size</p> $SD = \sqrt{\frac{\sum_{i=1}^{N_{patch}} (a_i - MPS)^2}{N_{patch}}}$ <ul style="list-style-type: none"> MPS: mean patch area size ai: area of patch i N_{patch}: number of patch | PADCV ≥ 0 | PADCV is zero when all patches in the landscape are the same size or there is only one patch (no variability in patch size). |
| 8 | Perimeter-Area Fractal Dimension PAFRAC | $\frac{N \sum_{i=1}^m \sum_{j=1}^n (\ln P_{ij} \cdot \ln a_{ij})}{\left(N \sum_{i=1}^m \sum_{j=1}^n \ln p_{ij}^2 \right) - \left(\sum_{i=1}^m \sum_{j=1}^n \ln p_{ij} \right)^2}$ <p>a_{ij} = area (m²) of patch ij. p_{ij} = perimeter (m) of patch ij. N = total number of patches in the landscape</p> | 1 ≤ PAFRAC ≤ 2 | It approaches 1 for shapes with very simple perimeters such as squares, and approaches 2 for shapes with highly convoluted, perimeters. PAFRAC requires patches to vary in size. |
| Category : Edge/border metrics | | | | |
| 9 | Edge density | $ED_k = \frac{\sum_{i=1}^n e_{ik}}{AREA} (10000)$ <p>k: patch type m: number of patch type n: number of edge segment of patch type k e_{ik}: total length of edge in landscape involving patch type k Area: total landscape area</p> | ED ≥ 0, without limit. ED = 0 when there is no class edge. | ED measures total edge of urban boundary used to compare landscape of varying sizes. |
| 10 | Area weighted mean patch fractal dimension (AWMPFD) | $AWMPFD = \frac{\sum_{i=1}^{i=N} 2 \ln 0.25 p_i / \ln S_i}{N} \times \frac{S_i}{\sum_{i=1}^{i=N} S_i}$ <p>Where s_i and p_i are the area and perimeter of patch i, and N is the total number of patches</p> | 1 ≤ AWMPFD ≤ 2 | AWMPFD approaches 1 for shapes with very simple perimeters, such as circles or squares, and approaches 2 for shapes with highly convoluted perimeter. AWMPFD describes the fragmentation of urban patches. If Sprawl is high then AWMPFD value is high. |
| 11 | Perimeter Area Weighted Mean Ratio. PARA_AM | $PARA_AM = \frac{P_{ij}}{A_{ij}}$ <p>P_{ij} = perimeter of patch ij A_{ij} = area weighted mean of patch ij</p> $AM = \sum_{j=1}^n [X_{ij} \left[\frac{a_{ij}}{\sum_{j=1}^n a_{ij}} \right]]$ | >0, without limit | PARA AM is a measure of fragmentation; it is a measure of the amount of 'edge' for a landscape or class. PARA AM value increased with increasing patch shape complexity. |
| 12 | A. Mean Patch Fractal Dimension (MPFD) | $B. \quad MPFD = \frac{\sum_{i=1}^m \sum_{j=1}^n \left(\frac{2 \ln(0.25 p_{ij})}{\ln a_{ij}} \right)}{N}$ <p>C. p_{ij} = perimeter of patch ij D. a_{ij} = area weighted mean of patch ij E. N = total number of patches in the landscape</p> | 1 ≤ MPFD < 2 | MPFD is another measure of shape complexity, approaches one for shapes with simple perimeters and approaches two when shapes are more complex. |

| | | | | |
|--|---|--|----------------------------------|--|
| 13 | Mean Patch Fractal Dimension (MPFD) coefficient of variation (COV) | $MPFD = \frac{\sum_{i=1}^m \sum_{j=1}^n \left(\frac{2 \ln(0.25 p_{ij})}{\ln a_{ij}} \right)}{N}$ $CV = \frac{SD}{MN} (100)$ <p>CV (coefficient of variation) equals the standard deviation divided by the mean, multiplied by 100 to convert to a percentage, for the corresponding patch metrics.</p> | It is represented in percentage. | It gives coefficient of variation of patches. |
| Category : Shape metrics | | | | |
| 14 | NLSI (Normalized Landscape Shape Index) | $NLSI = \frac{\sum_{i=1}^{i=N} P_i}{N S_i}$ <p>Where s_i and p_i are the area and perimeter of patch i, and N is the total number of patches.</p> | $0 \leq NLSI < 1$ | NLSI = 0 when the landscape consists of single square or maximally compact almost square, it increases when the patch types becomes increasingly disaggregated |
| 15 | Mean Shape index MSI | $MSI = \frac{\sum_{j=1}^n \left(\frac{0.25 p_{ij}}{\sqrt{a_{ij}}} \right)}{n_i}$ <p>p_{ij} is the perimeter of patch i of type j. a_{ij} is the area of patch i of type j. n_i is the total number of patches.</p> | MSI ≥ 1 , without limit | Explains Shape Complexity. MSI is equal to 1 when all patches are circular (for polygons) or square (for raster (grids)) and it increases with increasing patch shape irregularity |
| 16 | Area Weighted Mean Shape Index (AWMSI) | $AWMSI = \frac{\sum_{i=1}^{i=N} P_i / 4 \sqrt{s_i}}{N} \times \frac{s_i}{\sum_{i=1}^{i=N} s_i}$ <p>Where s_i and p_i are the area and perimeter of patch i, and N is the total number of patches</p> | AWMSI ≥ 1 , without limit | AWMSI = 0 when all patches in the landscape are circular or square. AWMSI increases without limit as the patch shape becomes irregular. |
| Category: Compactness/ contagion / dispersion metrics | | | | |
| 17 | Clumpiness | $CLUMPY = \left[\begin{array}{l} \frac{G_i - P_i}{P_i} \text{ for } G_i < P_i \text{ \& } P_i < 5, \text{ else} \\ \frac{G_i - P_i}{1 - P_i} \end{array} \right]$ $G_i = \left(\frac{g_{ii}}{\left(\sum_{k=1}^m g_{ik} \right) - \min e_i} \right)$ <p>g_{ii} =number of like adjacencies (joins) between pixels of patch type (class) i based on the <i>double-count</i> method. g_{ik} =number of adjacencies (joins) between pixels of patch types (classes) i and k based on the <i>double-count</i> method. $\min-e_i$ =minimum perimeter (in number of cell surfaces) of patch type (class) i for a maximally clumped class. P_i =proportion of the landscape occupied by patch type (class) i.</p> | $-1 \leq CLUMPY \leq 1$ | It equals 0 when the patches are distributed randomly, and approaches 1 when the patch type is maximally aggregated. |

| | | | | |
|--------------------------------------|---|--|----------------------------------|---|
| 18 | Area weighted Euclidean mean nearest neighbor distance AW_MNND | $ENN = h_{ij}$ <p>h_{ij} is distance (m) from patch ij to nearest neighboring patch of the same type(class) based on shortest edge to edge distance.</p> | ENN>0, without limit | ENN approaches zero as the distance to the nearest neighbor decreases. |
| 19 | ENND coefficient of variation | $ENN = h_{ij}$ $CV = \frac{SD}{MN}(100)$ <p>CV (coefficient of variation) equals the standard deviation divided by the mean, multiplied by 100 to convert to a percentage, for the corresponding patch metrics.</p> | It is represented in percentage. | In the analysis of urban processes, greater isolation indicates greater dispersion. |
| 20 | Aggregation index | $AI = \left[\sum_{i=1}^m \left(\frac{g_{ii}}{\max \rightarrow g_{ii}} \right) P_i \right] (100)$ <p>g_{ii}=number of like adjacencies (joins) between pixels of patch type (class) i based on the single count method.</p> | $1 \leq AI \leq 100$ | AI equals 1 when the patches are maximally disaggregated and equals 100 when the patches are maximally aggregated |
| 21 | Interspersion and Juxtaposition | $IJI = \frac{-\sum_{i=1}^m \sum_{k=i+1}^m \left[\left(\frac{e_{ik}}{E} \right) \cdot \ln \left(\frac{e_{ik}}{E} \right) \right]}{\ln(0.5[m(m-1)])} (100)$ <p>e_{ik} = total length (m) of edge in landscape between patch types (classes) i and k. E = total length (m) of edge in landscape, excluding background m = number of patch types (classes) present in the landscape, including the landscape border, if present.</p> | $0 \leq IJI \leq 100$ | IJI is used to measure patch adjacency. IJI approach 0 when distribution of adjacencies among unique patch types becomes increasingly uneven; is equal to 100 when all patch types are equally adjacent to all other patch types. |
| Category : Open Space metrics | | | | |
| 22 | Ratio of open space (ROS) | $ROS = \frac{s'}{s} \times 100\%$ <p>Where s is the summarization area of all "holes" inside the extracted urban area, s is summarization area of all patches</p> | It is represented as percentage. | The ratio, in a development, of open space to developed land. |
| 23 | Patch dominance | $Dominance = \ln(m) + \sum_{i=1}^m pi \ln(pi)$ <p>m: number of different patch type i: patch type; pi: proportion of the landscape occupied by patch type i</p> | ----- | Computes dominance's diversity index on a raster map. |

Appendix II:

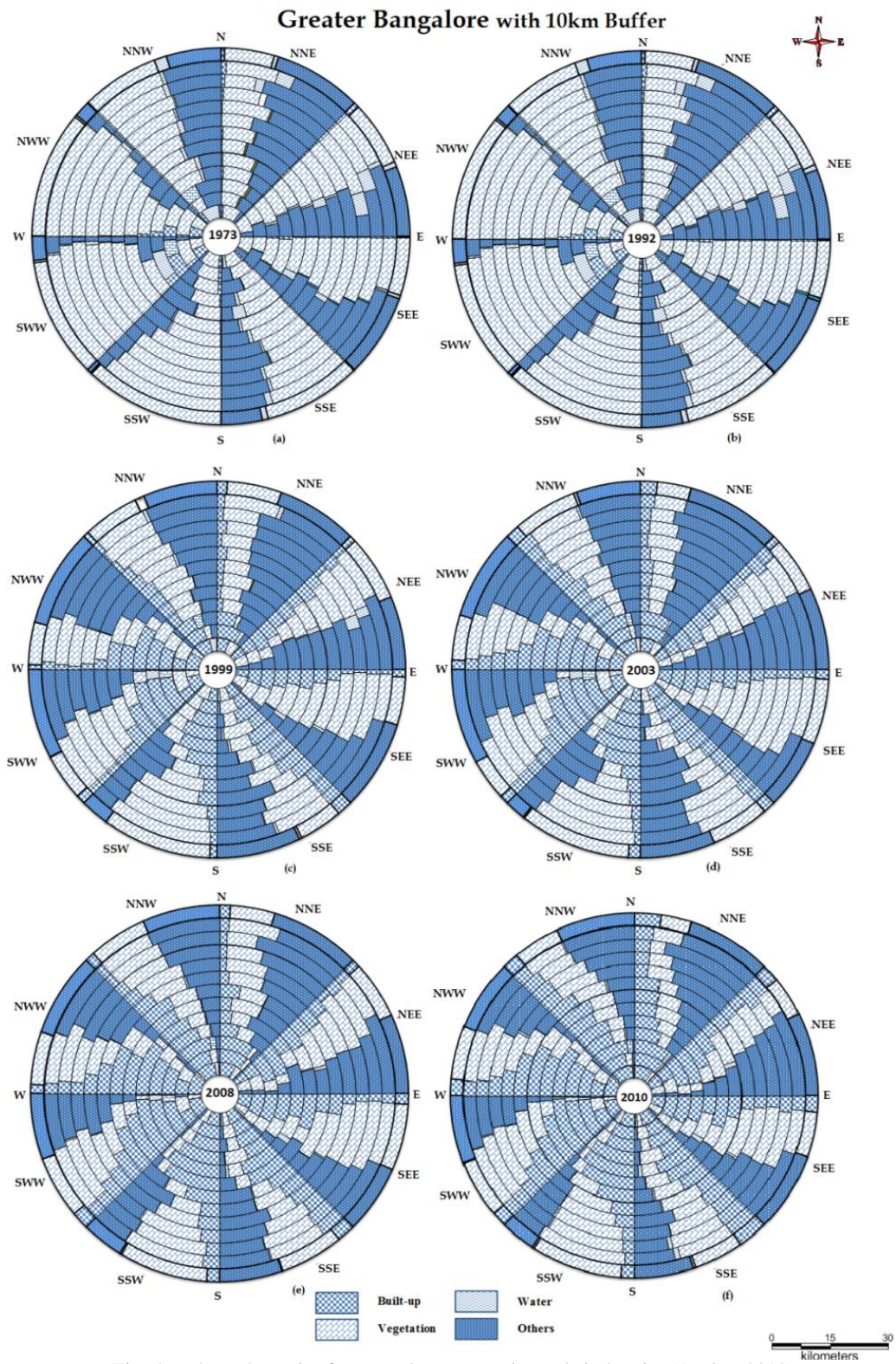


Fig. 6 Land use dynamics for Bangalore Zone-wise and circle-wise (1973 to 2010)

Appendix III:

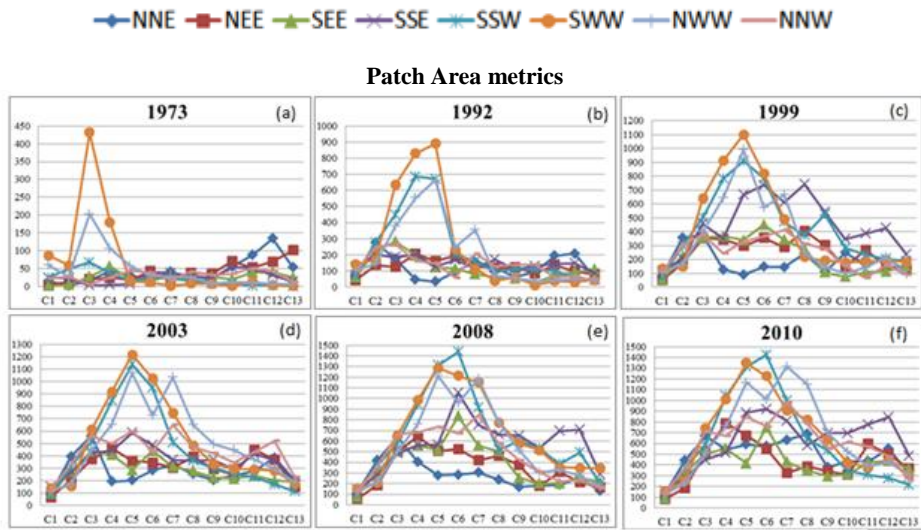


Fig. 7(a, b, c, d, e, f) Built-up area in Ha

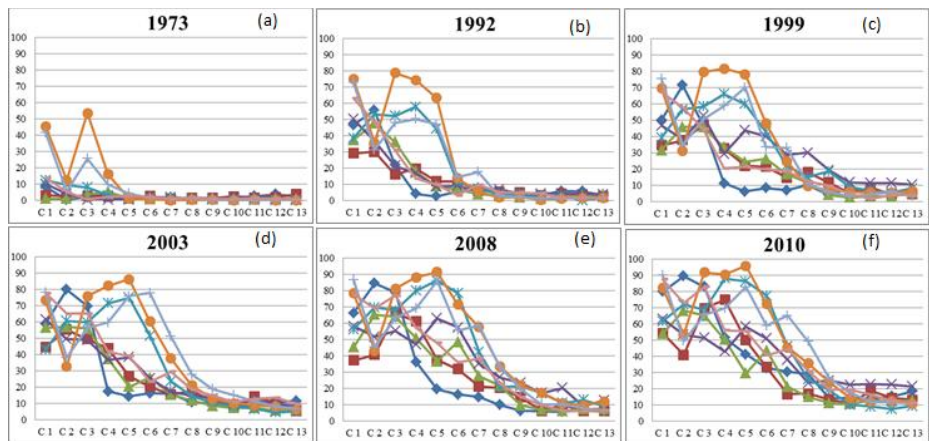


Fig. 8 (a, b, c, d, e, f) Built-up area in %

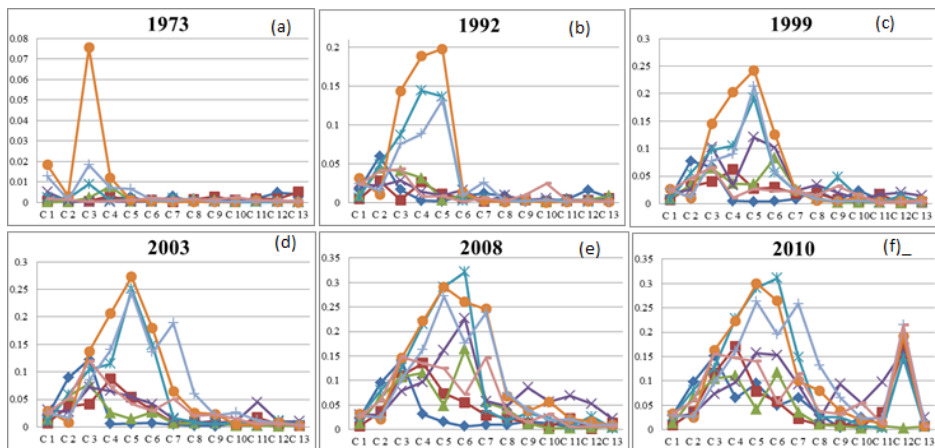


Fig. 9 (a, b, c, d, e, f) Largest Patch Index (Built-up area)

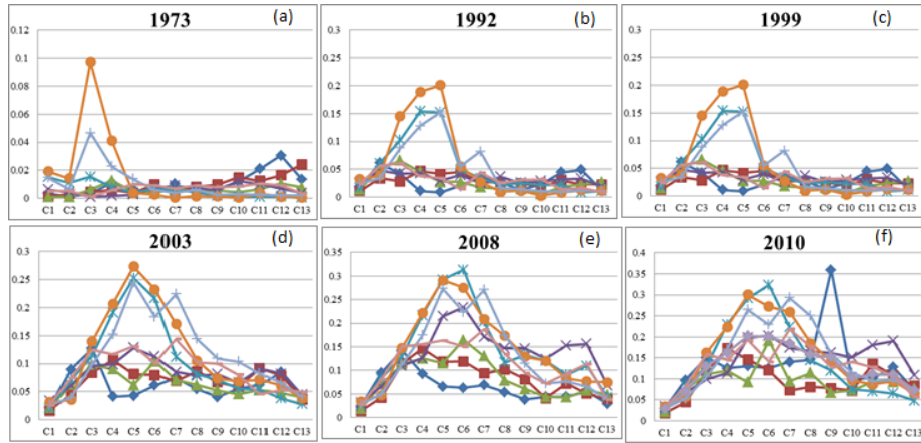


Fig. 10 (a, b, c, d, e, f) Largest Patch Index (landscape)

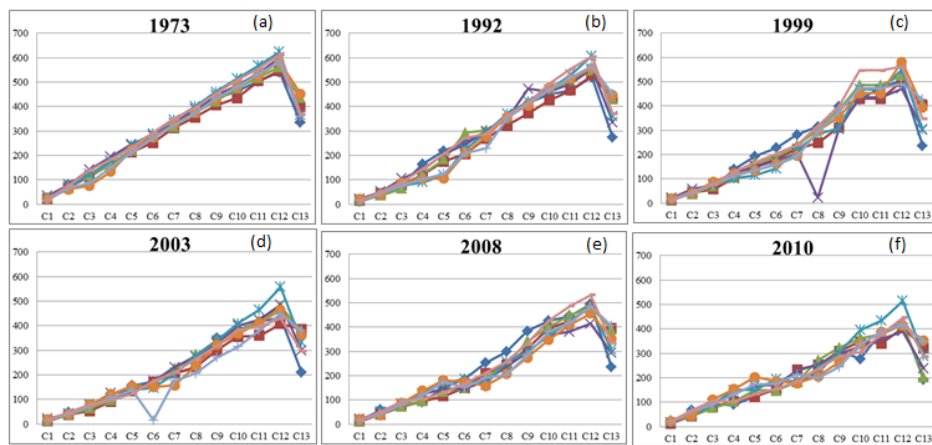


Fig. 11(a, b, c, d, e, f) Mean Patch Size

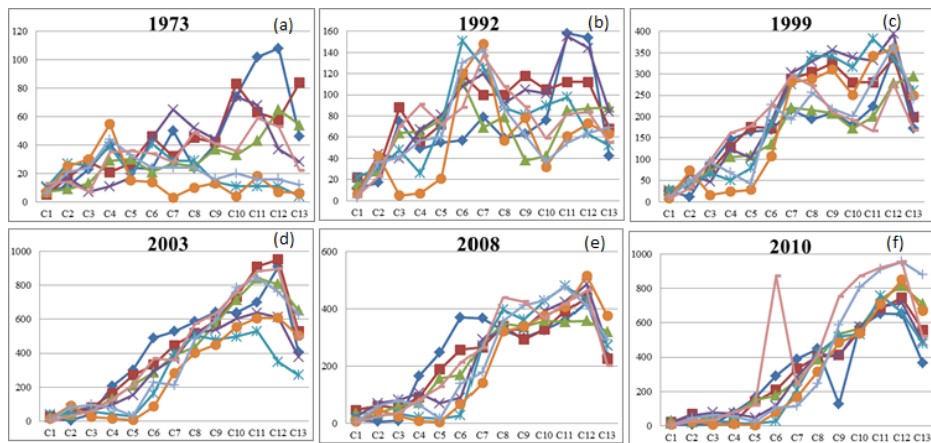


Fig. 12(a, b, c, d, e, f) Number of Patches (NP)

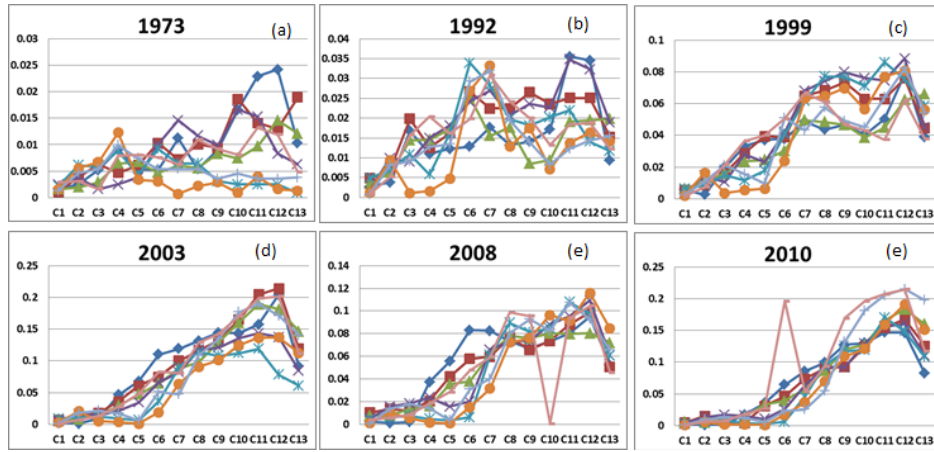


Fig. 13 (a, b, c, d, e, f) Patch Density (PD)

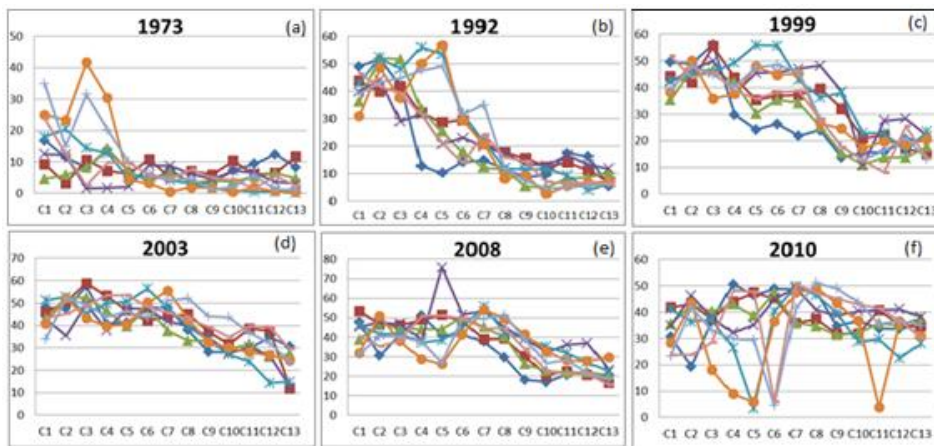


Fig. 14 (a, b, c, d, e, f) PADCVC

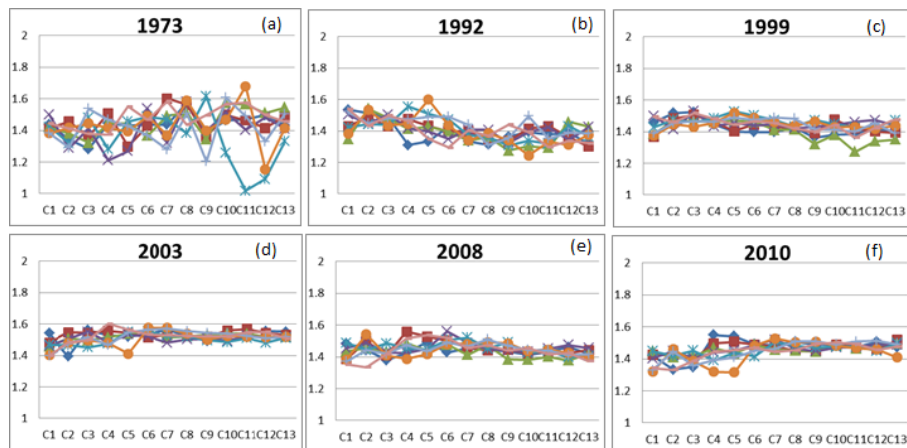


Fig. 15 (a, b, c, d, e, f) PAFRAC

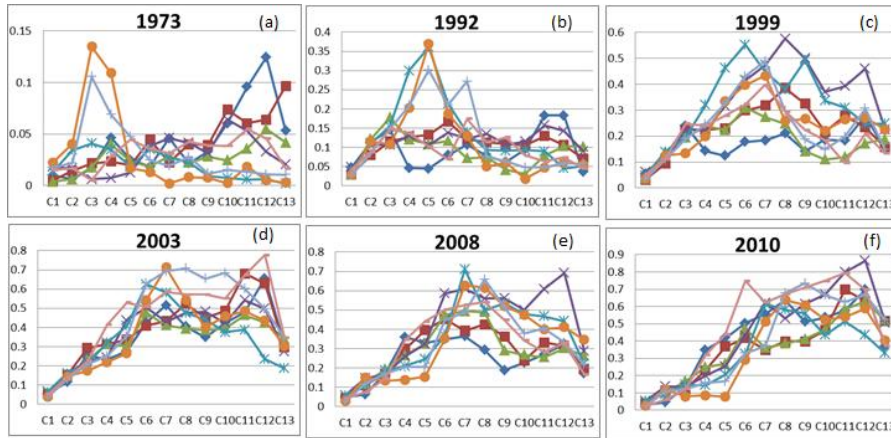


Fig. 16 (a, b, c, d, e, f) Edge Density(ED)

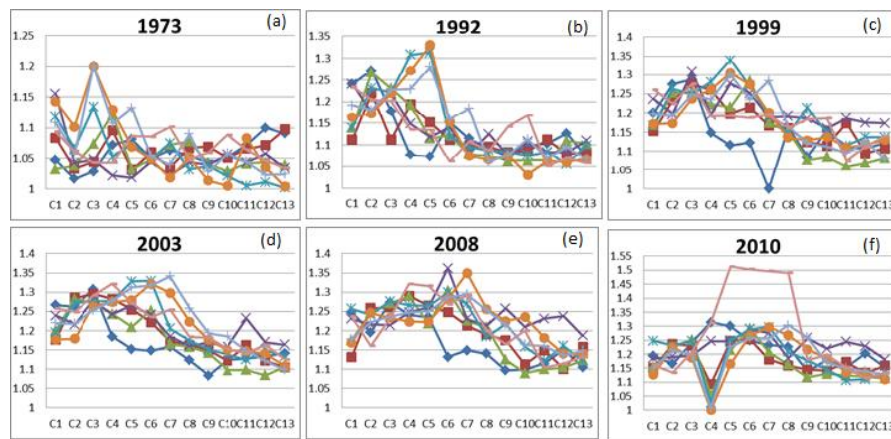


Fig. 17 (a, b, c, d, e, f) AWMPFD

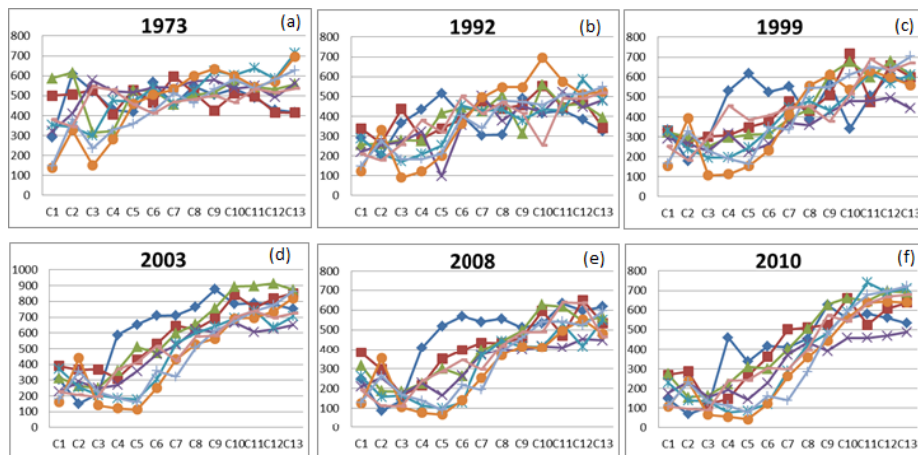


Fig. 18 (a, b, c, d, e, f) PARA_AM

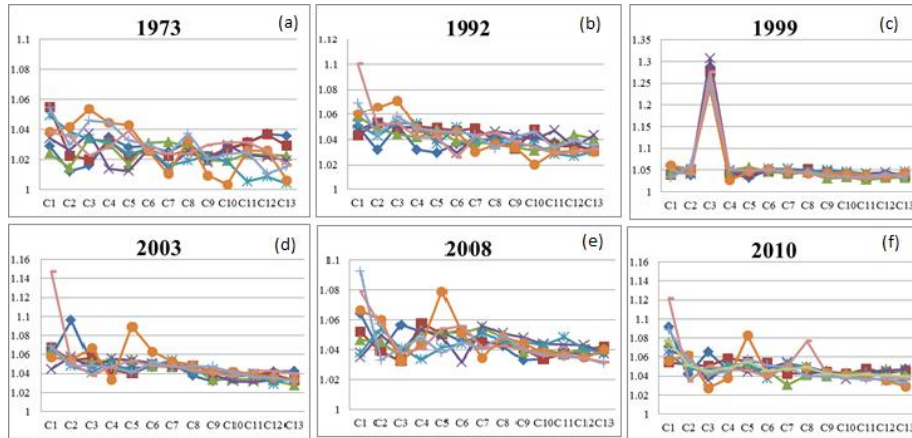


Fig. 19 (a, b, c, d, e, f) MPFD

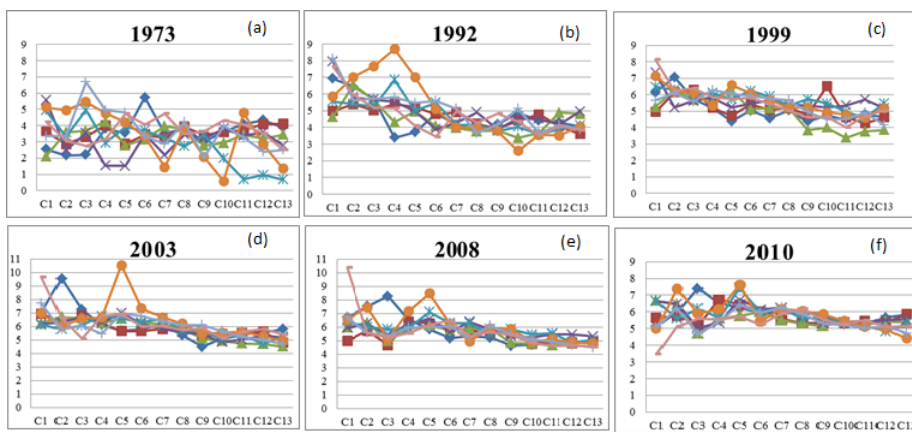


Fig. 20 (a, b, c, d, e, f) MPFD_CV

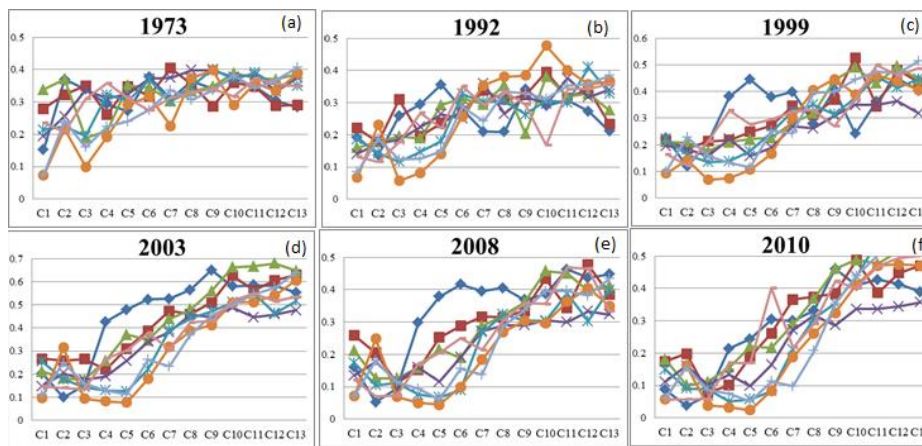


Fig. 21 (a, b, c, d, e, f) NLSI

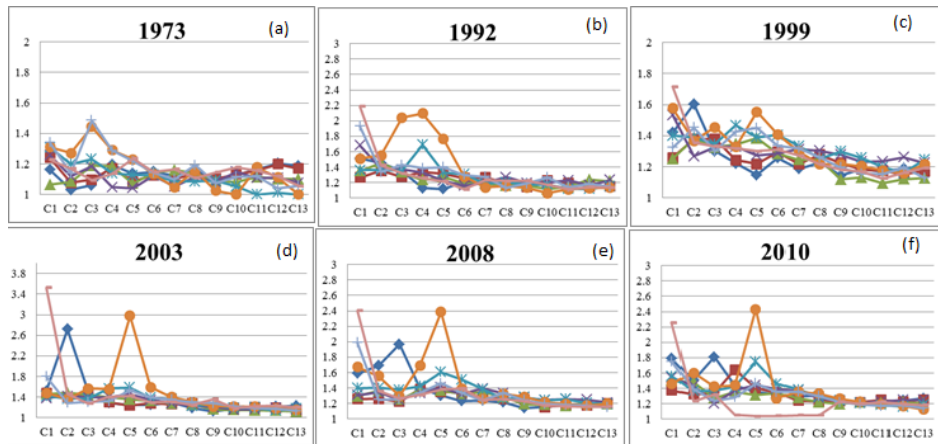


Fig. 22 (a, b, c, d, e, f) MSI

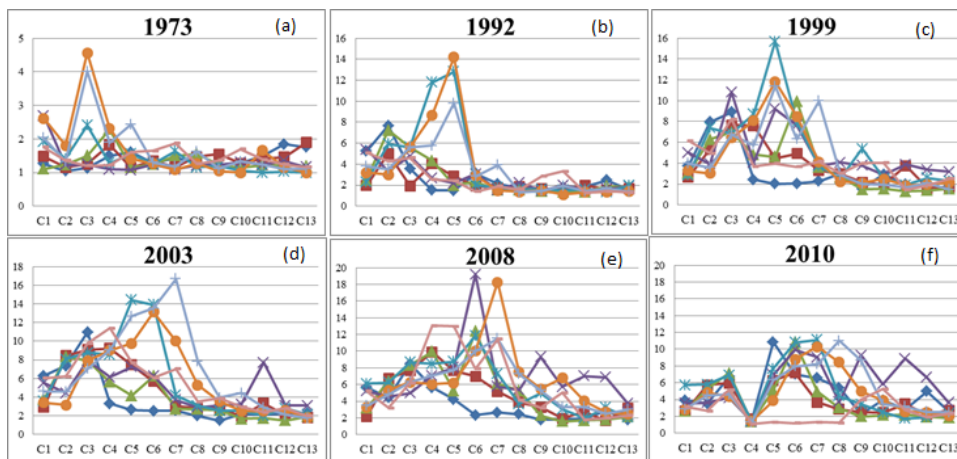


Fig. 23 (a, b, c, d, e, f) AWMSI

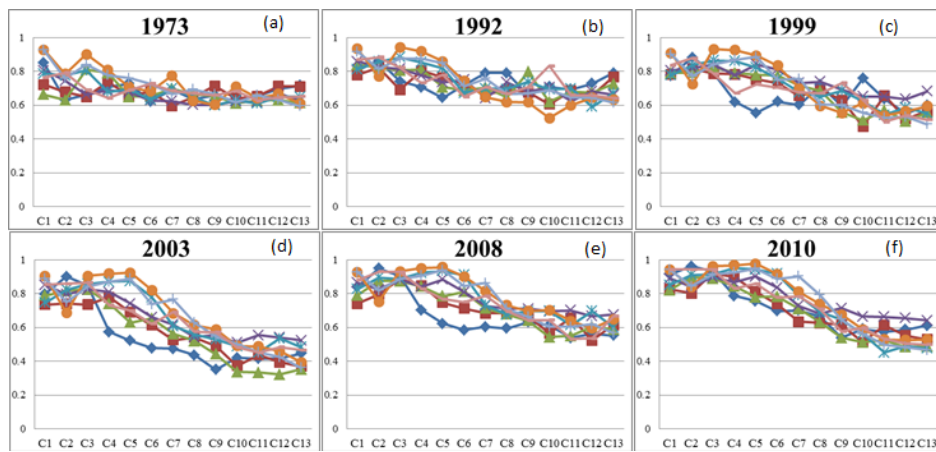


Fig. 24 (a, b, c, d, e, f) Clumpiness

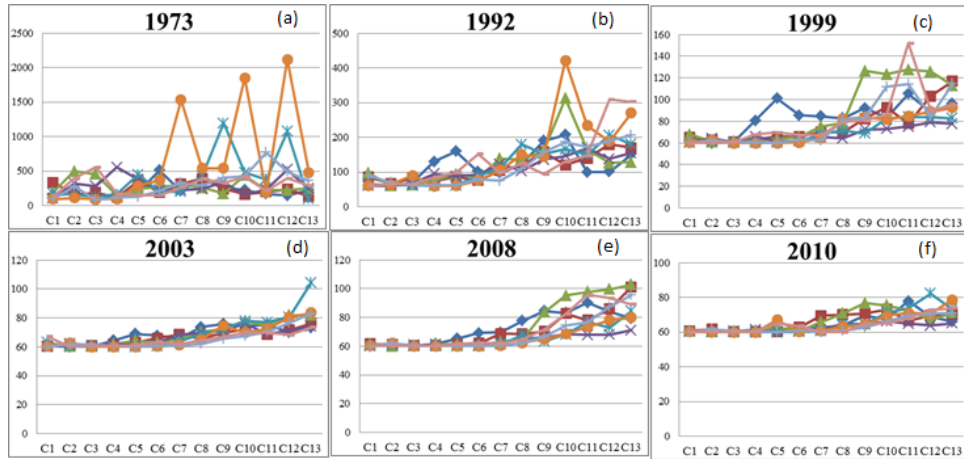


Fig. 25 (a, b, c, d, e, f) ENN_AM

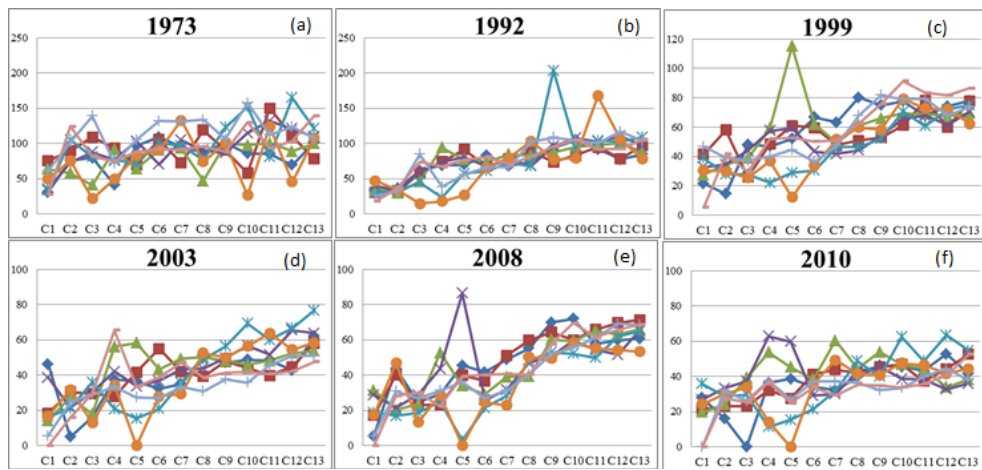


Fig. 26 (a, b, c, d, e, f) ENN_CV

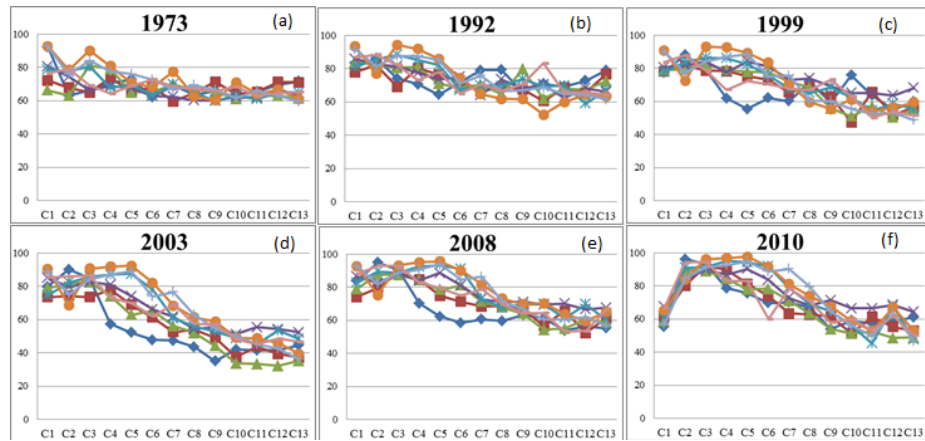


Fig. 27 (a, b, c, d, e, f) AI

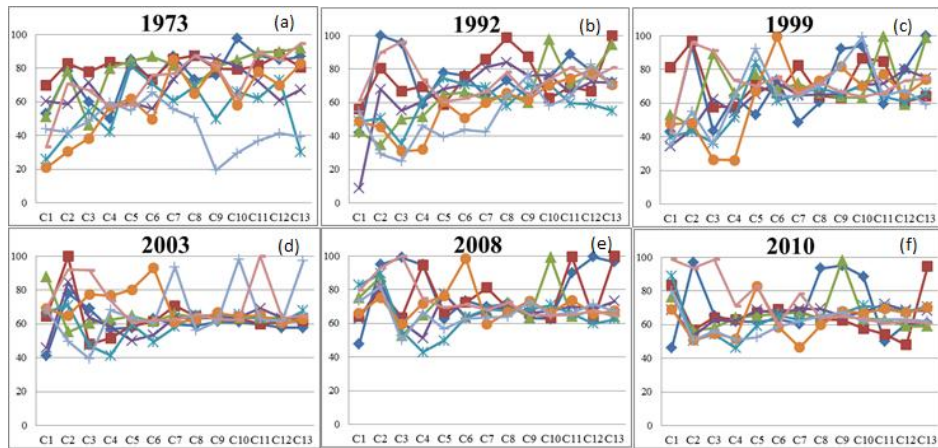


Fig. 28 (a, b, c, d, e, f) JJI

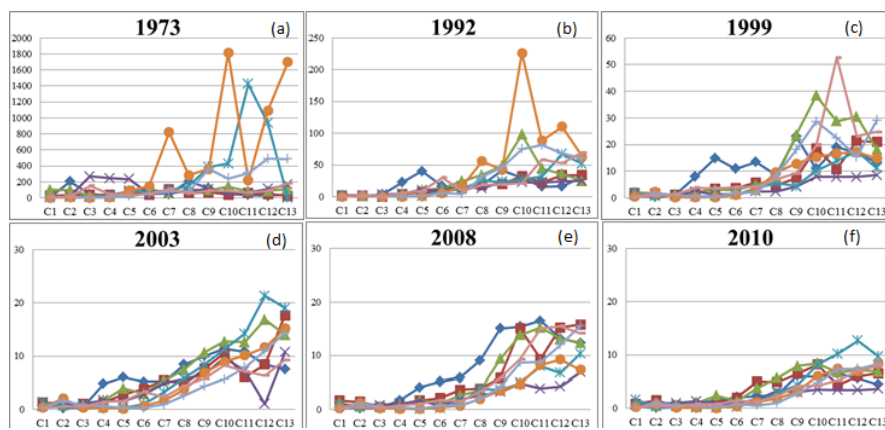


Fig. 29 (a, b, c, d, e, f) ROS

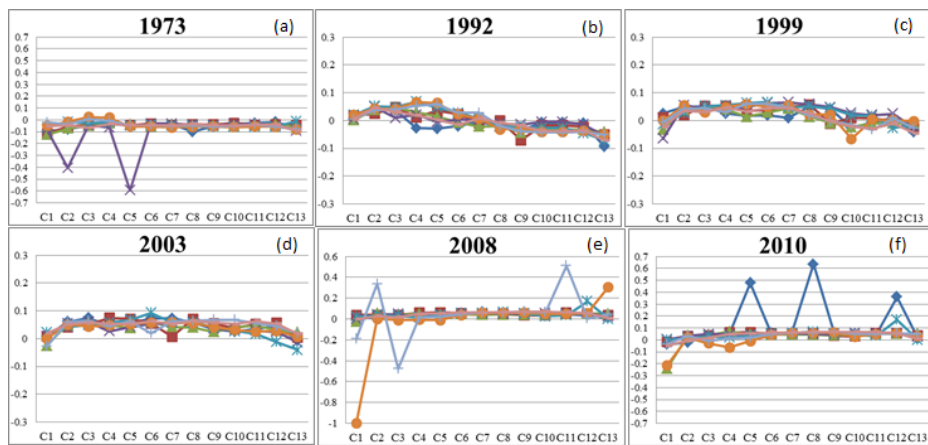


Fig. 30 (a, b, c, d, e, f) Dominance